PHILOSOPHICAL TRANSACTIONS A

royalsocietypublishing.org/journal/rsta

Research

Cite this article: Hartmann S, Ferri R, Bruni O, Baumert M. 2021 Causality of cortical and cardiovascular activity during cyclic alternating pattern in non-rapid eye movement sleep. *Phil. Trans. R. Soc. A* **379**: 20200248.
https://doi.org/10.1098/rsta.2020.0248

Accepted: 1 February 2021

One contribution of 17 to a theme issue 'Advanced computation in cardiovascular physiology: new challenges and opportunities'.

Subject Areas:
biomedical engineering

Keywords:
multivariate analysis, Granger causality, cyclic alternating pattern, network physiology, sleep microstructure

Author for correspondence:
Mathias Baumert
e-mail: mathias.baumert@adelaide.edu.au

Causality of cortical and cardiovascular activity during cyclic alternating pattern in non-rapid eye movement sleep

Simon Hartmann[1], Raffaele Ferri[2], Oliviero Bruni[3] and Mathias Baumert[1]

[1]School of Electrical and Electronic Engineering, University of Adelaide, Adelaide, Australia
[2]Sleep Research Center, Department of Neurology IC, Oasi Research Institute-IRCCS, Troina, Italy
[3]Department of Social and Developmental Psychology, Sapienza University, Rome, Italy

SH, 0000-0001-9689-0594; MB, 0000-0003-2984-2167

The dynamic interplay between central and autonomic nervous system activities plays a pivotal role in orchestrating sleep. Macrostructural changes such as sleep-stage transitions or phasic, brief cortical events elicit fluctuations in neural outflow to the cardiovascular system, but the causal relationships between cortical and cardiovascular activities underpinning the microstructure of sleep are largely unknown. Here, we investigate cortical–cardiovascular interactions during the cyclic alternating pattern (CAP) of non-rapid eye movement sleep in a diverse set of overnight polysomnograms. We determine the Granger causality in both 507 CAP and 507 matched non-CAP sequences to assess the causal relationships between electroencephalography (EEG) frequency bands and respiratory and cardiovascular variables (heart period, respiratory period, pulse arrival time and pulse wave amplitude) during CAP. We observe a significantly stronger influence of delta activity on vascular variables during CAP sequences where slow, low-amplitude EEG activation phases (A1) dominate than during non-CAP sequences. We also show that rapid, high-amplitude EEG activation phases (A3) provoke a more pronounced change in autonomic activity than A1 and A2 phases. Our analysis provides the first evidence on the causal

THE ROYAL SOCIETY PUBLISHING

interplay between cortical and cardiovascular activities during CAP. Granger causality analysis may also be useful for probing the level of decoupling in sleep disorders.

This article is part of the theme issue 'Advanced computation in cardiovascular physiology: new challenges and opportunities'.

1. Background

Sleep is a state of reduced consciousness that serves several purposes, including energy conservation, metabolic brain waste clearance, modulation of immune responses, memory consolidation and re-consolidation and preservation of mental well-being [1]. During sleep, the body is kept in homeostasis [2]; cortical and subcortical brain structures display rich dynamics orchestrating an array of physiological processes that affect the neural outflow to the cardiovascular system, among other things [3]. External triggers may perturb the cardiovascular system and, along with interoceptive processes, information may be relayed back to the brain, forming complex closed-loop control systems [4,5]. Traditionally, sleep is primarily scored by evaluating electroencephalography (EEG) activity, while chin muscle tone and eye movement may be added to distinguish rapid eye movement (REM) from non-REM (NREM) sleep [6]. The former is characterized by random rapid movements of the eyes while the latter exhibits three distinct stages that cover the transitions from high neuronal activity during light sleep to quiescence during deep sleep [7]. During REM sleep, the sympathetic activity intensifies but declines again below the level of wakefulness after transitioning to NREM sleep [8,9], causing hypotension and bradycardia [10]. The close relationship between central nervous system (CNS) activity and autonomic nervous system (ANS) activity during sleep is also apparent during phasic, transient events such as arousals or K-complexes [3]. Both heart rate and blood pressure are easily accessible markers of ANS activity and rise rapidly after the onset of sleep arousal, which is defined as the rapid shift from slow EEG waves to high frequencies in the α or β band [4,11]. K-complexes that are defined as synchronized phasic events principally found in the thalamocortical circuitry [12] demonstrate a biphasic pattern in the cardiac response, highlighting the association between the CNS and ANS [13].

A more comprehensive approach describing transient, phasic perturbations during sleep is cyclic alternating pattern (CAP) analysis. CAP consists of periodically recurring arousal-related phasic events called activation phases (A-phases) that interrupt the slow cortical activity of NREM sleep. CAP is defined a sequence of at least two consecutive cycles of an A-phase and the following background period (B-phase) terminated by an A-phase that is considered to be non-CAP [14]. By definition, A- and B-phases are restricted to intervals of 2–60 s. Typical patterns of A-phases include δ bursts, vertex sharp transients, K-complex sequences, K-alpha, polyphasic bursts, intermittent alpha and arousals [14]. A-phases can be categorized into three subtypes based on their dominant frequency component and EEG synchrony [15]. Subtype A1 represents high-voltage, slow waves with high EEG synchrony. On the contrary, A3 subtypes display low-amplitude, fast rhythms with low EEG synchrony [14]. Subtype A2 is defined as a mixture of both but is often merged with A3 into one subtype (A2 + 3) because of their congruent nature [16].

CAP is an important indicator of NREM sleep instability [17]. CAP combines information on CNS and ANS activity. CAP sequences represent continuing arousal oscillations [18], including the activating effect on the ANS such as heart rate and blood pressure [19], whereas non-CAP periods display sustained stability between the CNS and ANS [20]. Several studies have assessed the relationship between CAP and cardiovascular dynamics. Ferini-Strambi *et al.* [21] reported a significantly increased low-frequency component and significantly decreased high-frequency component of heart rate variability (HRV) during CAP compared with non-CAP in 10 healthy subjects. A study by Ferri *et al.* [22] of six normal children and adolescents supports the findings of altered sympathovagal balance. In their studies on HRV during CAP in healthy subjects and patients with nocturnal front lobe epilepsy (NFLE), Dorantes-Mendez *et al.* [23,24] demonstrated

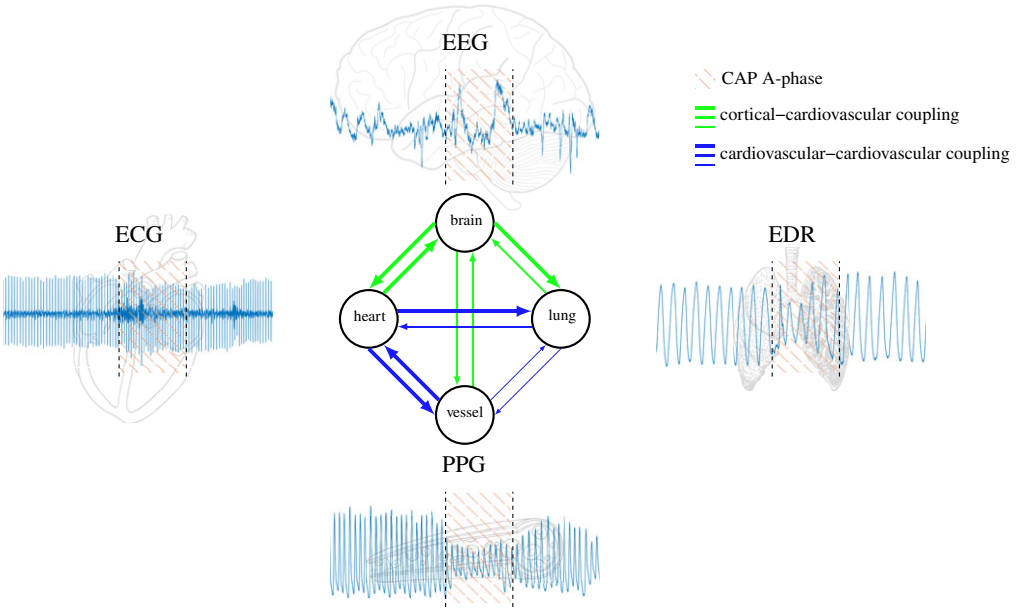

Figure 1. Schematic illustration of cortical and cardiovascular coupling investigated during cyclic alternating pattern (CAP) activation phases (A-phase). EEG, electroencephalography; ECG, electrocardiography; PPG, photoplethysmography; EDR, electrocardiogram-derived respiration. (Online version in colour.)

a comparable significant shift towards the low-frequency components of HRV with a more pronounced shift in A3-phases than in A1- and A2-phases. Furthermore, a study on the relation between EEG changes defined by A-phases and the pulse wave amplitude (PWA) after airway obstruction in patients with obstructive sleep apnoea demonstrates a significant correlation between respiratory events combined with A-phases and respiratory events combined with PWA drops [25]. In summary, these findings indicate significant sympathetic activity alterations underpinning the microstructure of sleep.

Physiological signals recorded non-invasively during sleep can be easily exploited to capture the coupling between cortical and autonomic activations. The signal-processing methods used to quantify these relationships range from multivariate linear and nonlinear techniques to entropy and information dynamics-based approaches [26]. Most studies investigate either the coupling between variables of autonomic functions such as HRV and blood pressure [27] or the interactions between the cortical and autonomic variables such as EEG frequency bands and HRV [28]. Faes *et al.* [29] used a wide spectrum of methods ranging from Wiener–Granger causality (GC) analysis to linear and nonlinear models [30] to an information-theoretic approach [31] to reveal causal interactions between brain–brain and brain–heart nodes during sleep. Novel methods use nonlinear convergent cross mapping [32] or the maximum information coefficient in combination with synthetic data generation models [33] to investigate the brain–heart interplay. Recently, the field of network physiology emerged with the objective of providing new insights into the dynamic interactions between multiple subsystems of the CNS and ANS [34,35]. This involves assembling hierarchical organizations for various physiological states based on the network interactions between brain waves and organs [36].

In this work, we report on causal relationships between cortical events defined by CAP and autonomic cardiovascular control; see figure 1. We determine brain activity using the energy in five EEG frequency bands and track autonomic activity changes based on electrocardiogram-derived respiration (EDR), heart period (HP), pulse arrival time (PAT) and PWA, the last two being closely related to arterial blood pressure changes. We use GC differences in

cortical–cardiovascular interactions during CAP sequences with predominantly A1-, A2- or A3-phases in comparison with non-CAP sequences.

2. Material and methods

(a) Database

We used data from the publicly available CAP Sleep Database on PhysioNet [14,37], which comprises 108 polysomnographic recordings conducted at the Sleep Disorders Center of the Ospedale Maggiore of Parma, Italy. Each recording contains at least three EEG channels, two electromyography channels, respiration signals and one electrocardiogram (ECG). Annotation files contain the scoring performed by expert neurologists, comprising sleep stages and CAP events according to the Rechtschaffen & Kales [6] rules and the atlas of CAP scoring [14], respectively. The dataset consists of recordings of 16 healthy subjects and 92 patients, including 40 subjects with NFLE (nfle), 22 with REM behaviour disorder (rbd), 10 with periodic leg movement (plm), 9 with insomnia (ins), 5 with narcolepsy (narco), 4 with sleep-disordered breathing (sdb) and 2 with bruxism (brux).

For our analysis, we selected recordings containing one central EEG channel (C4-A1), one ECG channel and one photoplethysmography (PPG) channel. The signal quality was reviewed and recordings with bad signal quality were removed to achieve congruent results. As a result, 55 patients were selected for our analysis (3 healthy, 4 ins, 3 narco, 28 nfle, 7 plm, 10 rbd). The included subjects were 43.3 ± 19.5 years old at the time of the recording with 40% being female. From each recording, we extracted the first three A-phases of each CAP sequence plus the preceding 30 s and the successive 10 s. If the fourth A-phase was located within the subsequent 10 s period, the sequence was removed. Furthermore, if the ECG channel or PPG channel segments were corrupted because of motion artefacts, the sequence was also removed. For each CAP sequence, a complementary non-CAP sequence of identical length and in the same sleep stage was extracted. In total, 507 sequences were extracted: 350 sequences with predominantly A1-phases, 78 sequences with predominantly A2-phases and 79 sequences with predominantly A3-phases. On average, each subject contributed 9.2 ± 5.4 sequences to the analysis. An example of a CAP sequence is displayed on the left side in figure 2.

(b) Signal processing

For each CAP and non-CAP sequence, we computed the EDR, HP, PAT and PWA using ECG and PPG. Prior to signal extraction, ECG and PPG were bandpass filtered using a finite impulse response (FIR) with a filter order of 20 and cut-off frequencies at 5–40 Hz and 0.5–20 Hz, respectively. EEG was not pre-processed prior to signal extraction because of the decomposition in five frequency bands with regards to the energy calculation. Because of missing thoracic or abdominal signals in the majority of selected subjects, we derived the respiratory waveform from ECG using the peak-to-trough QRS amplitude [38]. Subsequently, we removed outliers that were outside the range of mean value ± 2 s.d. in a sliding, non-overlapping 30 s window. The continuous EDR signal was computed using cubic spline interpolation with an interpolation interval of 0.25 s.

We defined HP as the R–R interval representing the time between two consecutive R peaks. We used the Pan–Tompkins algorithm for detection of R peaks in the ECG [39]. The timing of each R peak and the time gap between R peaks were subsequently used to determine the continuous HP signal using cubic spline interpolation with an interpolation interval of 0.25 s.

PAT quantifies the time a pulse wave takes from the heart to reach a distal site, mostly the fingertip. Commonly, the R peak in the ECG is selected as an approximation of the start, and the systolic peak in PPG is chosen as the end of the interval [40]. Here, we used the R peak and the time the PPG reaches two-thirds of the systolic peak as references for the calculation of PAT because a fiducial mark closer to half of the systolic upstroke is clinically more relevant as it

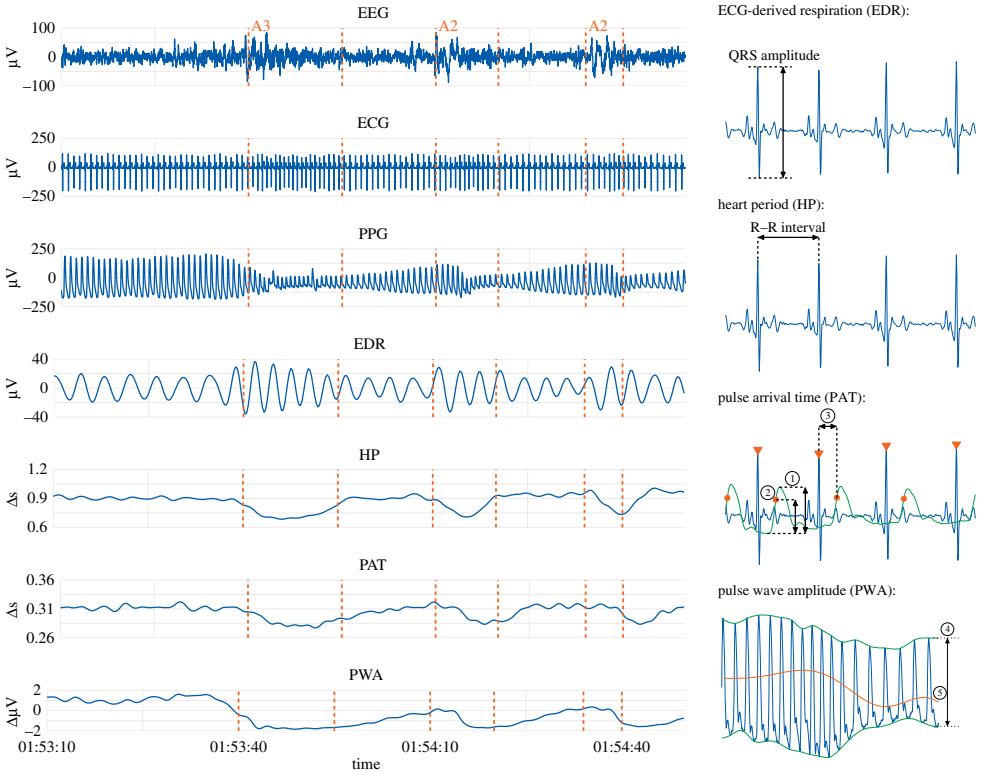

Figure 2. Example of a cyclic alternating pattern (CAP) sequence in the electroencephalogram (EEG) of subject plm9 including two A2-phases and one A3-phase plus the preceding 30 s and the subsequent 10 s (left side). The algorithms to determine electrocardiogram-derived respiration (EDR), heart period (HP), pulse arrival time (PAT) and pulse wave amplitude (PWA) in electrocardiography (ECG) and photoplethysmography (PPG) are illustrated on the right-hand side. EDR is determined based on the QRS amplitude, whereas HP is derived from the R–R interval. PAT ③ is computed as the period from the R peak to two-thirds ② of the systolic upstroke ①. PWA is defined as the amplitude difference ④ between the upper and lower envelope of the PPG and the subsequently normalized value ⑤. (Online version in colour.)

portrays the start point of the pulse wave propagation across the artery [41]. A continuous PAT signal was created by interpolating the discrete values of the time period between each R peak and its corresponding reference at the PPG waveform using cubic splines and an interpolation interval of 0.25 s.

We defined PWA as the amplitude difference between the systolic peak and its diastolic base in each pulse wave [42]. The upper envelope representing the systolic peaks was calculated using peak detection in a time span of 1/16 s and cubic spline interpolation with an interpolation interval of 0.25 s. The same approach was applied to determine the lower envelope. Consequently, we computed PWA as the difference between the upper and lower envelope and normalized it.

To capture cortical activity, we computed the energy in five EEG frequency bands: δ (0.5–4 Hz), θ (4–8 Hz), α (8–12 Hz), σ (12–16 Hz) and β (16–25 Hz). Two-way least-squares FIR filtering with a filter order of 3* (sample rate/low cut-off frequency) was used to decompose the EEG into its bands. The band energy for each sequence was defined as the sum of the squared magnitudes using non-overlapping windows of 0.25 s. All autonomic function and EEG variables were computed using a sample rate of 4 Hz. Furthermore, the autonomic variables were filtered using a bandpass filter with cut-off frequencies at 0.08 Hz and 0.4 Hz. Figure 2 illustrates the algorithms used to extract the aforementioned variables.

Moreover, we plotted the 10 s after plus the 5 s before each onset of the first A-phase in each extracted sequence to analyse the dynamic changes in brain and cardiovascular activity. For each

variable, we used the average of a 5 s time window before the start of the plot as a reference. We selected only the first A-phase of each CAP sequence to prevent any long-lasting influence of preceding A-phases.

(c) Granger causality

The GC was proposed by N. Wiener in 1956 and later formalized by Granger [43]. It is a very powerful and popular tool to estimate causal relationships and the directions of information propagation between the time series of a multivariate set. Over the years, GC has been extended to improve the accuracy of the causality prediction, including information and frequency domain methods [44]. Time series X_i is called the Granger cause to time series X_j if the prediction of X_j significantly improves in case the history of X_i is included [45].

Suppose $\boldsymbol{X}$ is a multivariate stochastic process with M scalar time series $X_1, \ldots, X_M$. Traditional GC analysis uses a vector autoregressive model (VAR) with a time lag of P

$$\boldsymbol{X}(n) = \sum_{k=1}^{P} \boldsymbol{A}(k)\boldsymbol{X}(n-k) + \boldsymbol{\epsilon}(n), \tag{2.1}$$

where $\boldsymbol{X}(n) = [X_1(n), \ldots, X_M(n)]^T$ contains the discrete samples of each time series at the time instant n, $\boldsymbol{A}(k)$ are $M \times M$ coefficient matrices and $\boldsymbol{\epsilon}$ are the residuals. In the first step of GC calculation, the VAR model in equation (2.1) is fitted to X_j, including the history of all time series in $\boldsymbol{X}$. The representation of the fitted VAR model with a time lag of P is given by

$$X_j(n) = \sum_{k=1}^{P} \boldsymbol{A}_j(k)\boldsymbol{X}(n-k) + \epsilon_j(n), \tag{2.2}$$

where $\boldsymbol{A}_j(k)$ is the coefficient matrix for time series X_j. In the next step, the VAR model in equation (2.1) is fitted to X_j, including the history of all time series in $\boldsymbol{X}$ except X_i. The resulting model estimates the contribution of X_i to the prediction of X_j

$$X_j(n) = \sum_{k=1}^{P} \boldsymbol{A}_j^*(k)\boldsymbol{X}_{/X_i}(n-k) + \epsilon_j^*(n), \tag{2.3}$$

where $\boldsymbol{X}_{/X_i}$ is the vector process without X_i, $\boldsymbol{A}_j^*$ contains the model coefficients and ϵ_j^* are the model residuals. Both $\boldsymbol{A}_j^*$ and ϵ_j^* are in general different from $\boldsymbol{A}_j(k)$ and ϵ_j in equation (2.2). Hence, the GC from X_i to X_j is defined as

$$\mathrm{GC}_{X_i \to X_j} = \ln \frac{\mathrm{var}(\epsilon_j^*(n))}{\mathrm{var}(\epsilon_j(n))}, \tag{2.4}$$

where $\epsilon_j^*(n)$ and $\epsilon_j(n)$ are the prediction errors and the $\mathrm{var}(\cdot)$ operator is the statistical variance. $\mathrm{GC}_{X_i \to X_j}$ is always positive and only describes the causal effects $X_i \to X_j$, which are independent from any other time series and from the reversed relationship $X_j \to X_i$.

For our analysis, we used the Matlab® toolbox developed by Schiatti *et al.* [46]. We decided to use the traditional GC method provided in the toolbox instead of the extended GC method as instantaneous causal relations are not expected in our analysis. The model order was selected according to the Bayesian information criterion (BIC) within the range 1–20, minimizing the BIC figure of merit.

(d) Statistical methods

We conducted Wilcoxon signed-rank tests to determine significant differences in GC between CAP and non-CAP segments (significance level: $p < 0.01$). Moreover, we assessed statistically significant non-zero GC values by comparing $\epsilon_j^*(n)$ and $\epsilon_j(n)$ using the Fisher F-test (significance level: $p < 0.01$) [47]. Prior to the F-test, we verified that the requirement of a normal distribution is

given by conducting the Kolmogorov–Smirnov test. In case the distribution was non-normal, we transformed the non-normally distributed data using Box–Cox transformation.

3. Results

(a) A-phase onset analysis

The changes in brain activity and autonomic variables before and after the first A-phase onset in each CAP sequence are summarized in figures 3–5, respectively. Figure 3 contains the plots for CAP sequences starting with an A1-phase (350 sequences) whereas figures 4 and 5 illustrate the course of change for CAP sequences starting with an A2- or A3-phase, respectively (78 and 79 sequences, respectively). For each CAP sequence, we extracted an equivalent non-CAP segment to compare the physiological behaviour between CAP and non-CAP periods.

After the onset of the first A1-phase in a CAP sequence, δ energy demonstrates a steep incline (highest median: 229.5% at 1.25 s after onset) whereas δ activity in non-CAP sequences remains stable across the time window. Differences in energy after the onset of an A1-phase can also be seen in the θ band (highest median: 96.5% at 0.50 s after onset). PWA indicates a change after the A1-phase onset as compared with non-CAP periods with a steady decline to −43.1% at 8.00 s. PAT displays a similar behaviour, reaching its valley at 7.25 s (−1.0%), whereas HP appears to start declining before the onset and reaches its minimum earlier than PWA and PAT (lowest median: −2.2% at 2.75 s before onset). No changes in autonomic cardiovascular activation can be seen in non-CAP periods. Respiration does not display notable changes.

Similar patterns in the EEG frequency bands can be seen after the onset of A2-phases (highest median for δ: 591.3% at 0.50 s after onset) but with more energy distributed in the θ and α frequency bands compared with A1-phases (highest median for θ: 177.0% at 0.25 s after onset, the highest median for α: 118.4% at 0.25 s after onset). All cardiovascular variables declined following the onset of an A2-phase, whereas they remain stable in non-CAP sequences. HP reaches its valley of −3.2% at 4.25 s after onset whereas PAT and PWA steadily decline to −1.4% and −112.7%, respectively, at 7.50 s and 8.50 s, respectively.

In line with A1- and A2-phases, δ energy demonstrates the highest increase among the EEG frequency bands after the onset of the first A3-phase (highest median for δ: 300.9% at 0.50 s after onset). Among high-frequency bands, the increase in energy is reasonably evenly distributed (71.9–123.5%), but β energy displays a delayed peak at 1.25 s. No substantial changes in any frequency band occur during non-CAP sequences across the time window (−13.9% to 15.4%). The three cardiovascular variables have a more pronounced decline following the onset of an A3-phase when compared with the other two subtypes; in particular, PWA demonstrates a steep decline with a minimum of −190.4% at 8.25 s. Furthermore, HP and PAT reach their valleys of −3.8% and −2.3%, respectively, at 4.25 s and 7.75 s, respectively.

(b) Causality analysis

Figures 6–8 display the results of the GC analysis for CAP sequences where A1-phases dominate (350 sequences with at least two A1-phases), sequences where A2-phases dominate (78 sequences with at least two A2-phases) and sequences where A3-phases dominate (79 sequences with at least two A3-phases).

During CAP sequences with predominant A1-phases, cortical activity appears to have a more pronounced causal impact on the autonomic activity than the reverse direction. In particular, δ activity plays a major role in CAP sequences with predominantly A1-phases as it demonstrates a high GC value throughout all nodes. Figure 6 shows a significantly higher $\delta \rightarrow$ PAT and $\delta \rightarrow$ PWA interaction during CAP periods than during non-CAP periods ($p < 0.001$). A larger number of $\delta \rightarrow$ PAT and $\delta \rightarrow$ PWA GC connections were statistically significant in CAP sequences with predominantly A1-phases than in non-CAP segments ($\delta \rightarrow$ PAT: 27% in CAP versus 21% in non-CAP, $\delta \rightarrow$ PWA: 41% in CAP versus 29% in non-CAP).

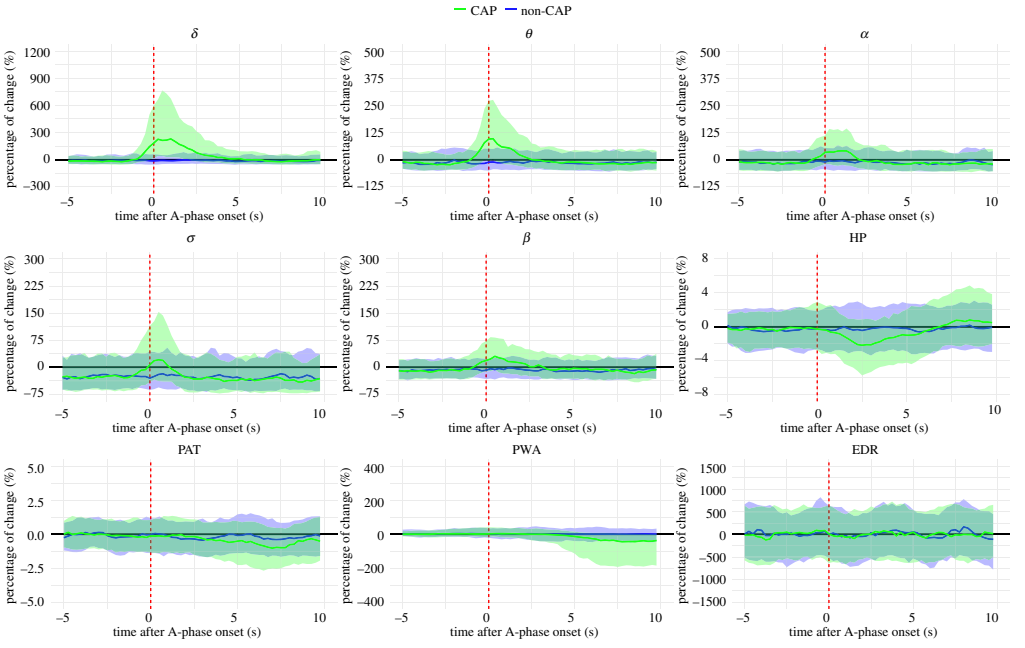

Figure 3. Summary of relative changes in electroencephalography frequency bands and autonomic functions (heart period (HP), pulse arrival time (PAT), pulse wave amplitude (PWA) and electrocardiogram-derived respiratory (EDR)) after the onset of an A1-phase initiating a cyclic alternating pattern (CAP) sequence as compared with non-CAP periods. Each plot displays the median and the 25th and 75th percentiles of 350 A1-phases. (Online version in colour.)

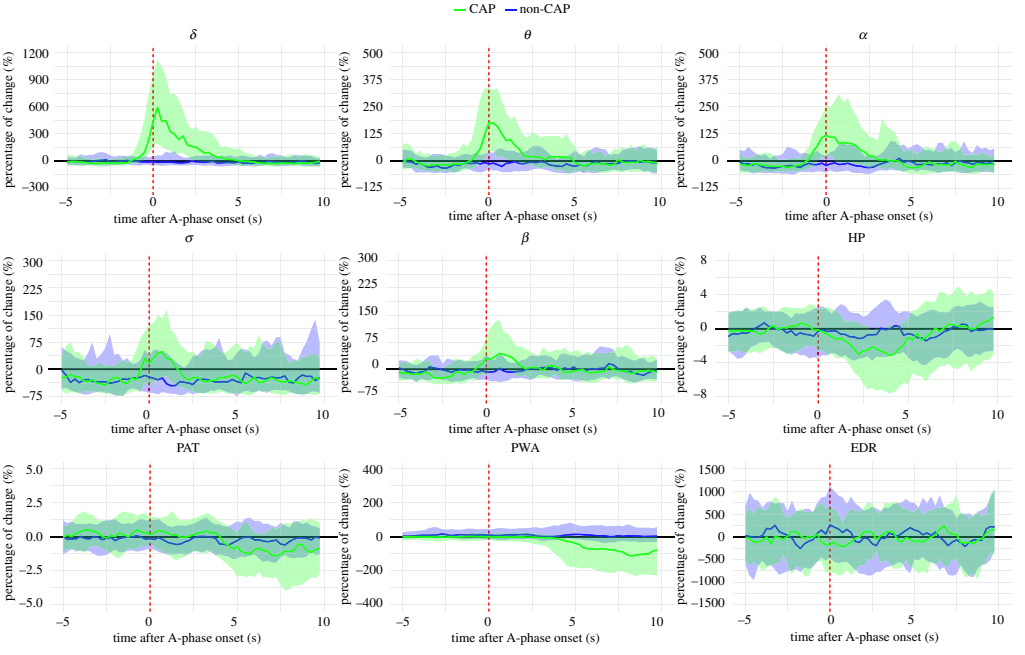

Figure 4. Summary of relative changes in electroencephalography frequency bands and autonomic functions (heart period (HP), pulse arrival time (PAT), pulse wave amplitude (PWA) and electrocardiogram-derived respiratory (EDR)) after the onset of an A2-phase initiating a cyclic alternating pattern (CAP) sequence as compared with non-CAP periods. Each plot displays the median and the 25th and 75th percentiles of 78 A2-phases. (Online version in colour.)

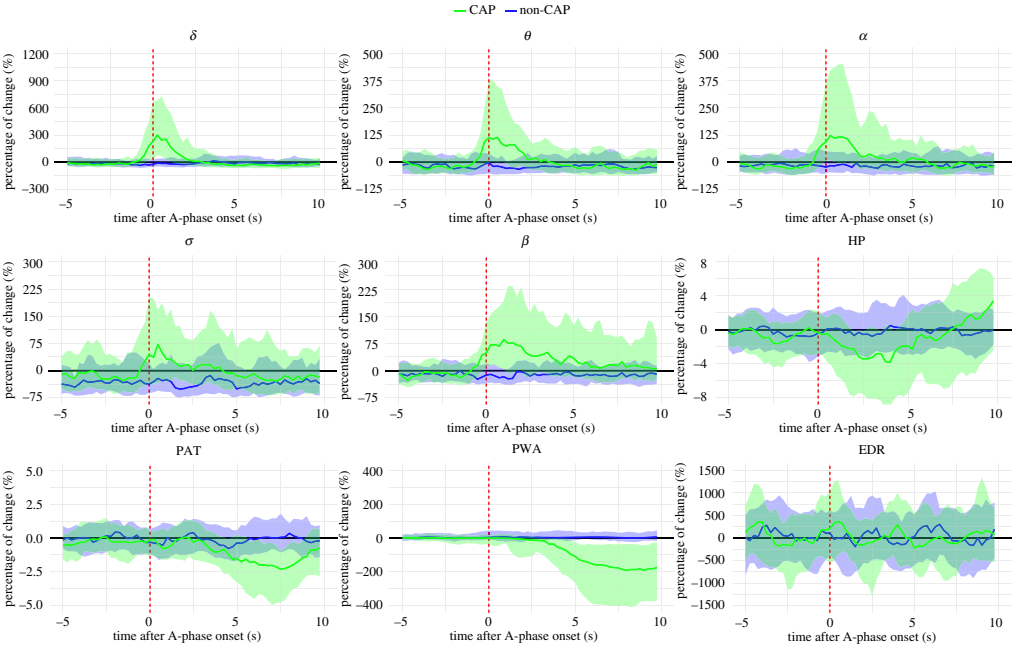

Figure 5. Summary of relative changes in electroencephalography frequency bands and autonomic functions (heart period (HP), pulse arrival time (PAT), pulse wave amplitude (PWA) and electrocardiogram-derived respiratory (EDR)) after the onset of an A3-phase initiating a cyclic alternating pattern (CAP) sequence when compared with non-CAP periods. Each plot displays the median and the 25th and 75th percentiles of 79 A3-phases. (Online version in colour.)

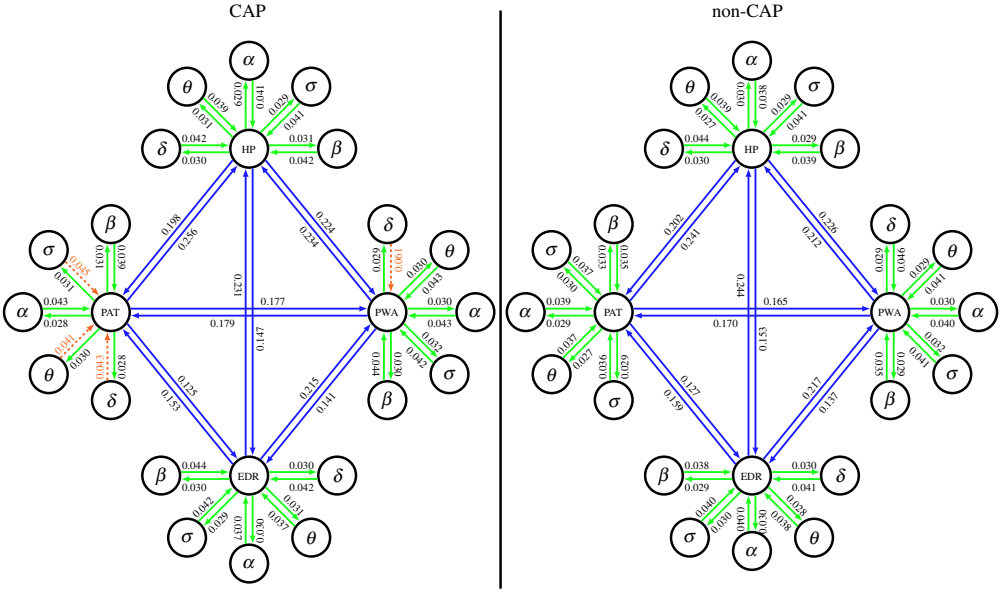

Figure 6. Graph of Wiener–Granger causality (GC) interactions between cortical–cardiovascular and cardiovascular–cardiovascular nodes. GC values for cyclic alternating pattern (CAP) sequences with predominantly A1-phases are shown on the left; GC values for equivalent non-CAP periods are shown on the right. Each connection displays the GC value averaged across all 350 sequences. Inner connections represent cortical–cardiovascular coupling and outer connections describe cardiovascular–cardiovascular coupling. Dashed connections demonstrate a significant difference in GC between CAP and non-CAP at a significance level of $p < 0.01$. HP, heart period; PAT, pulse arrival time; PWA, pulse wave amplitude; EDR, electrocardiogram-derived respiration. (Online version in colour.)

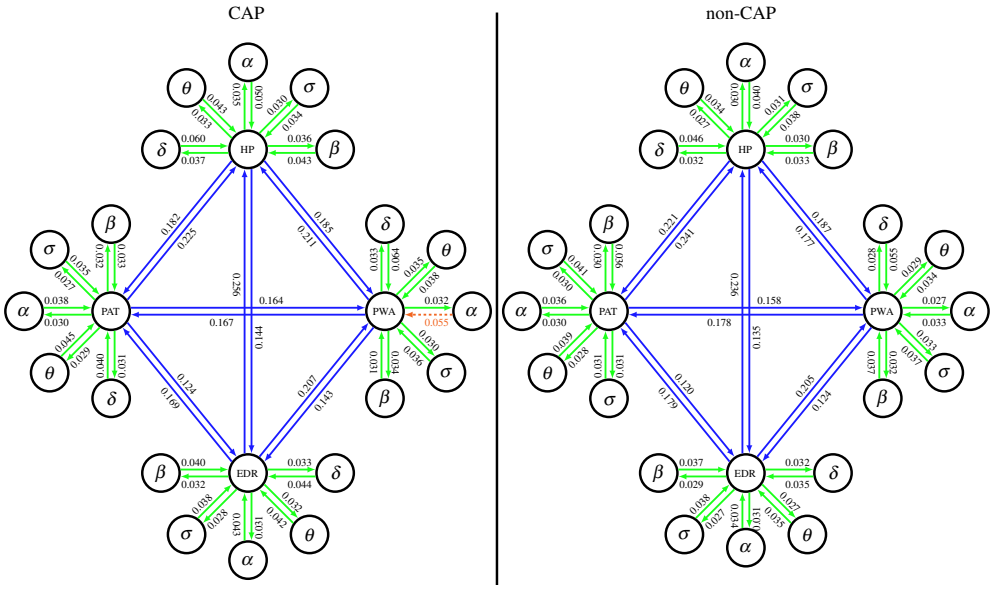

Figure 7. Graph of Wiener–Granger causality (GC) interactions between cortical-cardiovascular and cardiovascular–cardiovascular nodes. GC values for cyclic alternating pattern (CAP) sequences with predominantly A2-phases are shown on the left; GC values for equivalent non-CAP periods are shown on the right. Each connection displays the GC value averaged across all 78 sequences. Inner connections represent cortical–cardiovascular coupling and outer connections describe cardiovascular–cardiovascular coupling. Dashed connections demonstrate a significant difference in GC between CAP and non-CAP at a significance level of $p < 0.01$. HP, heart period; PAT, pulse arrival time; PWA, pulse wave amplitude; EDR, electrocardiogram-derived respiration. (Online version in colour.)

Additionally, PAT appears to be significantly more influenced by $\boldsymbol{\theta}$ and $\boldsymbol{\sigma}$ during CAP segments than during non-CAP segments ($p < 0.001$), with 29% and 29%, respectively, of the sequences indicating a significant GC connection (non-CAP: 19% and 23%, respectively).

Figure 7 displays the relation between cortical activity and autonomic activity for CAP periods with predominantly A2-phases. Similar to sequences with predominantly A1-phases, cortical activity appears to have a more substantial impact on autonomic activity than vice versa. Of note, figure 7 shows a significant difference for the $\boldsymbol{\alpha} \rightarrow$ PWA interactions during CAP periods with predominantly A2-phases than during non-CAP periods ($p = 0.008$), where approximately one-third of all $\boldsymbol{\alpha} \rightarrow$ PWA interactions in CAP sequences demonstrated a significant non-zero GC (non-CAP: 17%). No further significant differences between CAP periods with predominantly A2-phases and non-CAP were found.

On the contrary, autonomic activity appears to have a stronger causal impact on cortical activity during CAP sequences with predominantly A3-phases than vice versa. Figure 8 displays a significantly higher PWA $\rightarrow \boldsymbol{\beta}$ interaction during CAP periods than during non-CAP periods ($p < 0.001$). Approximately one-quarter of all sequences demonstrated a significant non-zero GC value for PWA $\rightarrow \boldsymbol{\beta}$ connections during CAP sequences with predominantly A3-phases, as compared with 11% during non-CAP periods.

4. Discussion

In this study, we show that short bursts of cortical $\boldsymbol{\delta}$ activity reflected by A1-phases cause an increase in vascular activity during sleep, which is likely to provoke a surge in arterial blood pressure. This suggests that A1-phases represent cortical events that, importantly, are not covered by the conventional American Sleep Disorders Association (ASDA) arousal definition [48] but

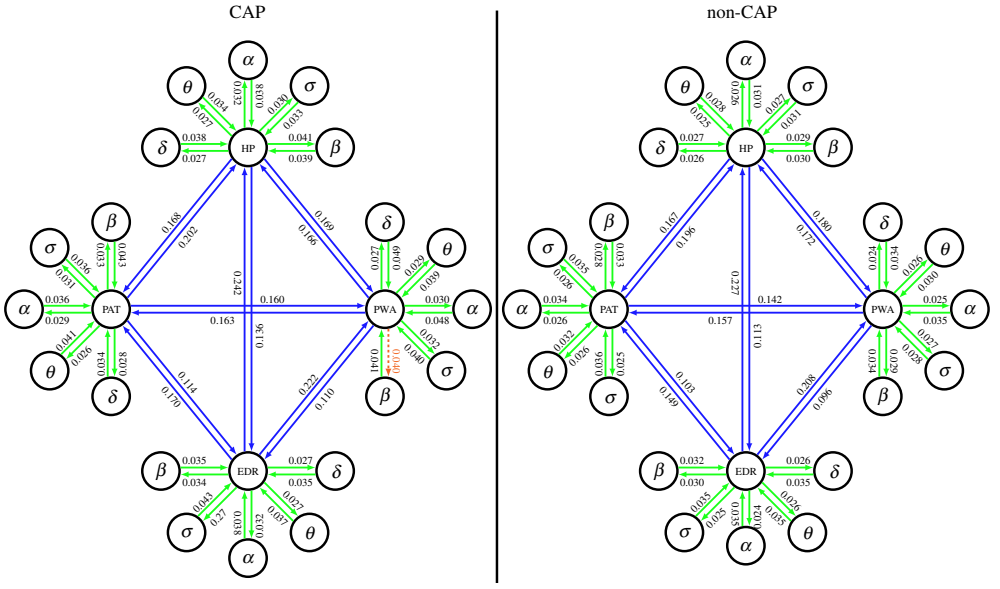

Figure 8. Graph of Wiener–Granger causality (GC) interactions between cortical–cardiovascular and cardiovascular–cardiovascular nodes. GC values for cyclic alternating pattern (CAP) sequences with predominantly A3-phases are shown on the left; GC values for equivalent non-CAP periods are shown on the right. Each connection displays the GC value averaged across all 79 sequences. Inner connections represent cortical–cardiovascular coupling and outer connections describe cardiovascular–cardiovascular coupling. Dashed connections demonstrate a significant difference in GC between CAP and non-CAP at a significance level of $p < 0.01$. HP, heart period; PAT, pulse arrival time; PWA, pulse wave amplitude; EDR, electrocardiogram-derived respiration. (Online version in colour.)

are responsible for arousal-like autonomic activations. Rapid, low-amplitude events defined as A3-phases appear to be preceded by increased autonomic activity. Moreover, a more pronounced impact on autonomic functions can be seen during A3-phases when compared with the other two subtypes.

Ensemble-average analysis of the onset of the initial A-phase in CAP sequences reveals a sudden increase in $\boldsymbol{\delta}$ and $\boldsymbol{\theta}$ activity during A1-phases. At the onset of A3-phases, all frequency bands display elevated energy levels with $\boldsymbol{\delta}$ and $\boldsymbol{\theta}$ activity rising prior to the onset of the A3-phase, whereas $\boldsymbol{\beta}$ activity peaks later during the A3-phase. This is in agreement with the CAP atlas [14], which specifies A1-phases as rhythms with more than 80% slow-wave activity whereas A3-phases contain a higher percentage of fast rhythms but with 50% of slow-wave activity at the beginning of the A-phase. Also, our analysis demonstrates a more pronounced effect on autonomic variables after the onset of A3-phases when compared with A1- and A2-phases. The minimum of HP and PWA after the onset of an A3-phase is substantially lower than after an A1-phase (HP: −2.2% after A1 versus −3.8% after A3, PWA: −43.1% after A1 versus −190.4% after A3) and PAT displays a slightly lower minimum for A3-phases (PAT: −1.0% after A1 versus −2.3% after A3). This supports the findings of previous studies [23,49] and is in line with the original definition of A-phases.

As A1-phases are defined in the CAP atlas as arousal equivalents and comprise K-complexes and $\boldsymbol{\delta}$ bursts [14], they can be categorized as subcortical or autonomic arousals. Sforza *et al.* [50] showed in their study that $\boldsymbol{\delta}$ bursts and K-complexes induce similar arousal responses as microarousals or phases of transitory activation [50]. However, the latter arousal types show an increase in heart rate prior to the arousal onset, whereas the increase in heart rate for $\boldsymbol{\delta}$ bursts and K-complexes appeared with a short latency. Our results corroborate these findings and demonstrate a clear causal connection between the $\boldsymbol{\delta}$ activity in A1-phases and the preceding sympathetic activation. In 27% and 41%, respectively, of the 350 CAP sequences with at least two

A1-phases, the shift in δ energy most likely Granger-causes a surge in blood pressure, resulting in a shorter PAT and a drop in PWA, respectively. Consequently, our findings provide further evidence that A1-phases are closely linked to an increase in sympathetic activity. However, the impact on autonomic functioning is less pronounced than for A3-phases.

Additionally, our GC analysis reveals a significant difference in the PWA $\rightarrow \beta$ interaction during CAP periods with predominantly A3-phases than during non-CAP periods. This could potentially be a result of the fact that spontaneous arousals show cardiovascular activation prior to the first signs of arousal in the EEG [51,52]. Such an increase in cardiovascular activity can be caused by external perturbations as CAP can be triggered by external conditions [17]. On the other hand, as a high percentage of arousals are preceded by slow waves such as K-complexes [53], ASDA arousals do not take into account the slow element of the double EEG activation (slow and rapid) that is typical in NREM sleep [54]. Thus, autonomous activations could be erroneously allocated before the onset of cortical activation [55] by not considering the pre-arousal slow-wave component. In our analysis, 22.8% of the CAP sequences with at least two A3-phases contained an A1-phase prior to an A3-phase, which is remarkably similar to the number of sequences with significant non-zero GC values for PWA $\rightarrow \beta$ interactions (24%). Hence, a preceding burst in delta activity may be the cause of the activation of the autonomic system, which in turn foreshadows a shift in energy towards higher frequencies in brain activity.

In our study, we investigated subjects of both genders with different sleep pathologies and this might influence the results. However, we should consider that the neural mechanisms that constitute CAP are independent of gender or sleep pathologies since it has been demonstrated that these factors modulate the quantitative aspects of CAP but not its intrinsic generation mechanisms [56]. Studies have demonstrated that the physiological fluctuations of CAP are accompanied by subtle, but significant, changes in the balance between the sympathetic and vagal components of the autonomic system in different age groups [22] and in pathological patients who present similar changes in the dynamics of the heart rate reflected by the modification of A-phase dynamics [57]. Another study reported an increase in heart rate with higher values of low-frequency power in the A-phases with no differences between healthy subjects and patients with epilepsy [24]. All these studies demonstrate that the neural mechanisms of CAP related to the heart–brain axis are independent from sleep pathologies.

One limitation of our study is the assessment of cortical–cardiovascular interactions using traditional GC analysis. The application of GC requires wide-sense stationary data [45], which are commonly not given in physiological signals such as EEG and HRV. One suggested approach is to shorten the analysed time segments [58]. The analysed sequences in this study represent a short fraction of an overnight recording and thus can be assumed locally stationary. Additionally, traditional GC analysis as it is applied in this study is based on linear regression models, which do not capture nonlinear effects. The assessment of nonlinear effects can be achieved with nonlinear GC methods such as kernel-based methods [59] or with transfer entropy as an information-theoretic causality measure [30]. Moreover, previous studies have shown that linear models work extremely well in neuroscience applications [60] and can detect similar brain–heart networks to nonlinear models in normal undisturbed sleep [30]. Additionally, the modelling of nonlinear systems using linear VAR systems can be sufficiently achieved by increasing the order of the fitted model adequately [61]. Finally, it is important to note the limitations of the GC measure. GC fails to measure an underlying causal mechanism, but it measures a causal effect, which is the reduction in prediction error [62]. Hence, the significant cortical–cardiovascular interactions detected in this study do not represent underlying anatomical connections, but they reflect the directed influence from one system to another [63]. For a more detailed decomposition of the reduction in prediction error similar to the information-theoretic assessment, extended frameworks of the predictability framework allow accounting for the influence from the target process itself, from other processes in the network and from the interaction with other processes [64].

One additional limitation of our study is the small number of recordings available in the CAP Sleep Database. A larger number of subjects resulting in a greater number of investigated

sequences would enable a more comprehensive analysis of the interplay between CNS and ANS during CAP. A possible solution is presented by automated CAP scoring algorithms that are capable of scoring large cohort studies [65–67]. Furthermore, the lack of healthy subjects in our analysis and the combination of various sleep pathologies is potentially limiting the significance of the presented results. However, the limited number of recordings with the required polysomnographic channels of each pathology in the CAP Sleep Database prevented a more in-depth analysis of the interaction of CNS and ANS for each subcategory. Hence, our study can only provide a general insight into the dynamic interplay of CNS and ANS during CAP. Finally, another limitation is the age distribution of the investigated dataset with mostly middle-aged or older subjects. As the CAP rate follows a U-shaped curve with a high number of A1-phases in young people and a high number of A2 + 3-phases in older people [68], the interplay between CNS and ANS during A-phase subtypes may also change throughout different age groups. We demonstrated in this study that the delta activity in A1-phases is the cause for activation of autonomic functions in middle-aged to older subjects. However, the rate of A1 subtypes is low in these age groups compared with younger subjects. In children, A1-phases are regarded as 'anti-arousals' [69] and support the homeostatic process to maintain the restorative function of sleep [70]. Hence, additional studies on the interplay between CNS and ANS during CAP in children could highlight differences in the autonomic response and the connection between delta activity and autonomic functions in children.

5. Conclusion

GC analysis between cortical and cardiovascular activation during CAP in NREM sleep demonstrates the important role of CAP in the assessment of physiological states during sleep. We show that A1-phases in CAP sequences, in particular the burst in delta activity, are closely linked to an increase in vascular activity during NREM sleep. We also show that A3-phases have a more pronounced impact on autonomic functions than A1- and A2-phases. These findings highlight the importance of sleep microstructure when evaluating autonomic activity alteration during sleep. Furthermore, we demonstrate the potential of GC analysis for gaining further information on CAP.

Data accessibility. All data in this study are available for free download from public repositories. The CAP Sleep Database can be downloaded from physionet.org.

Authors' contributions. S.H. conceived and designed the study, carried out the experiments, performed the data analysis and drafted the manuscript. M.B. conceived and designed the study, and performed the data analysis. O.B. and R.F. contributed to the analysis and interpretation of the data. All authors read and approved the manuscript.

Competing interests. We declare we have no competing interests.

Funding. This study was partly supported by a grant from the Australian Research Council (grant no. DP0663345).

References

1. Zielinski MR, McKenna JT, McCarley RW. 2016 Functions and mechanisms of sleep. *AIMS Neurosci.* **3**, 67–104. (doi:10.3934/Neuroscience.2016.1.67)
2. Benington JH. 2000 Sleep homeostasis and the function of sleep. *Sleep* **23**, 959–966. (doi:10.1093/sleep/23.7.1j)
3. de Zambotti M, Trinder J, Silvani A, Colrain I, Baker FC. 2018 Dynamic coupling between the central and autonomic nervous systems during sleep: a review. *Neurosci. Biobehav. Rev.* **90**, 84–103. (doi:10.1016/j.neubiorev.2018.03.027)
4. Silvani A, Calandra-Buonaura G, Benarroch EE, Dampney RAL, Cortelli P. 2015 Bidirectional interactions between the baroreceptor reflex and arousal: an update. *Sleep Med.* **16**, 210–216. (doi:10.1016/j.sleep.2014.10.011)
5. Silvani A, Dampney RAL. 2013 Central control of cardiovascular function during sleep. *Am. J. Physiol. Circ. Physiol.* **305**, H1683–H1692. (doi:10.1152/ajpheart.00554.2013)

6. Rechtschaffen A, Kales A. 1968 *A manual for standardized terminology, techniques and scoring system for sleep stages in human subjects*. Los Angeles, CA: Brain Information Service/Brain Research Institute.
7. Iber C, Ancoli-Israel S, Chesson A, Quan S. 2007 *The AASM manual for the scoring of sleep and associated events: rules, terminology and technical specifications*. Westchester, IL: American Academy of Sleep Medicine.
8. Somers VK, Dyken ME, Mark AL, Abboud FM. 1993 Sympathetic-nerve activity during sleep in normal subjects. *N. Engl. J. Med.* **328**, 303–307. (doi:10.1056/NEJM199302043280502)
9. Trinder J, Kleiman J, Carrington M, Smith S, Breen S, Tan N, Kim Y. 2001 Autonomic activity during human sleep as a function of time and sleep stage. *J. Sleep Res.* **10**, 253–264. (doi:10.1046/j.1365-2869.2001.00263.x)
10. Mancia G. 1993 Autonomic modulation of the cardiovascular system during sleep. *N. Engl. J. Med.* **328**, 347–349. (doi:10.1056/NEJM199302043280511)
11. Trinder J, Allen N, Kleiman J, Kralevski V, Taylor D, Anson K, Kim Y. 2003 On the nature of cardiovascular activation at an arousal from sleep. *Sleep* **26**, 543–551. (doi:10.1093/sleep/26.5.543)
12. Amzica F, Steriade M. 2002 The functional significance of K-complexes. *Sleep Med. Rev.* **6**, 139–149. (doi:10.1053/smrv.2001.0181)
13. de Zambotti M, Willoughby AR, Franzen PL, Clark DB, Baker FC, Colrain IM. 2016 K-complexes: interaction between the central and autonomic nervous systems during sleep. *Sleep* **39**, 1129–1137. (doi:10.5665/sleep.5770)
14. Terzano MG *et al.* 2001 Atlas, rules, and recording techniques for the scoring of cyclic alternating pattern (CAP) in human sleep. *Sleep Med.* **2**, 537–553. (doi:10.1016/s1389-9457(01)00149-6)
15. Terzano MG, Parrino L. 2000 Origin and significance of the cyclic alternating pattern (CAP). *Sleep Med. Rev.* **4**, 101–123. (doi:10.1053/smrv.1999.0083)
16. Smerieri A, Parrino L, Agosti M, Ferri R, Terzano MG. 2007 Cyclic alternating pattern sequences and non-cyclic alternating pattern periods in human sleep. *Clin. Neurophysiol.* **118**, 2305–2313. (doi:10.1016/j.clinph.2007.07.001)
17. Parrino L, Ferri R, Bruni O, Terzano MG. 2012 Cyclic alternating pattern (CAP): the marker of sleep instability. *Sleep Med. Rev.* **16**, 27–45. (doi:10.1016/j.smrv.2011.02.003)
18. Terzano MG, Parrino L, Spaggiari MC. 1988 The cyclic alternating pattern sequences in the dynamic organization of sleep. *Electroencephalogr. Clin. Neurophysiol.* **69**, 437–447. (doi:10.1016/0013-4694(88)90066-1)
19. Kondo H *et al.* 2014 Association between heart rate variability, blood pressure and autonomic activity in cyclic alternating pattern during sleep. *Sleep* **37**, 187–194. (doi:10.5665/sleep.3334)
20. Parrino L, Milioli G, Melpignano A, Trippi I. 2016 The cyclic alternating pattern and the brain-body-coupling during sleep. *Epileptologie* **33**, 150–160.
21. Ferini-Strambi L, Bianchi A, Zucconi M, Oldani A, Castronovo V, Smirne S. 2000 The impact of cyclic alternating pattern on heart rate variability during sleep in healthy young adults. *Clin. Neurophysiol.* **111**, 99–101. (doi:10.1016/S1388-2457(99)00212-6)
22. Ferri R, Parrino L, Smerieri A, Terzano MG, Elia M, Musumeci SA, Pettinato S. 2000 Cyclic alternating pattern and spectral analysis of heart rate variability during normal sleep. *J. Sleep Res.* **9**, 13–18. (doi:10.1046/j.1365-2869.2000.00190.x)
23. Dorantes-Méndez G, Mendez MO, Alba A, Parrino L, Milioli G. 2018 Time-varying analysis of the heart rate variability during A-phases of sleep: healthy and pathologic conditions. *Biomed. Signal Process. Control* **40**, 111–116. (doi:10.1016/j.bspc.2017.09.010)
24. Dorantes G, Méndez M, Alba A, González JS, Parrino L, Milioli G. 2015 Heart rate variability in cyclic alternating pattern during sleep in healthy and nocturnal front lobe epilepsy patients. In *Proc. of the Annu. Int. Conf. of the IEEE Engineering in Medicine and Biology Society, EMBS, Milan, Italy, 25–29 August 2015*, pp. 5944–5947. IEEE.
25. Bosi M, Milioli G, Riccardi S, Melpignano A, Vaudano AE, Cortelli P, Poletti V, Parrino L. 2018 Arousal responses to respiratory events during sleep: the role of pulse wave amplitude. *J. Sleep Res.* **27**, 261–269. (doi:10.1111/jsr.12593)
26. Pereda E, Quiroga RQ, Bhattacharya J. 2005 Nonlinear multivariate analysis of neurophysiological signals. *Prog. Neurobiol.* **77**, 1–37. (doi:10.1016/j.pneurobio.2005.10.003)

27. Silvani A *et al.* 2008 Sleep-dependent changes in the coupling between heart period and blood pressure in human subjects. *Am. J. Physiol. Integr. Comp. Physiol.* **294**, R1686–R1692. (doi:10.1152/ajpregu.00756.2007)
28. Jurysta F, van de Borne P, Migeotte P-F, Dumont M, Lanquart J-P, Degaute J-P, Linkowski P. 2003 A study of the dynamic interactions between sleep EEG and heart rate variability in healthy young men. *Clin. Neurophysiol.* **114**, 2146–2155. (doi:10.1016/S1388-2457(03)00215-3)
29. Faes L, Marinazzo D, Jurysta F, Nollo G. 2014 Granger causality analysis of sleep brain-heart interactions. In *Proc. 2014 8th Conf. of the European Study Group on Cardiovascular Oscillations (ESGCO), Trento, Italy, 25–28 May 2014*, pp. 5–6. IEEE.
30. Faes L, Marinazzo D, Jurysta F, Nollo G. 2015 Linear and non-linear brain-heart and brain-brain interactions during sleep. *Physiol. Meas.* **36**, 683–698. (doi:10.1088/0967-3334/36/4/683)
31. Faes L, Nollo G, Jurysta F, Marinazzo D. 2014 Information dynamics of brain-heart physiological networks during sleep. *N. J. Phys.* **16**, 105005. (doi:10.1088/1367-2630/16/10/105005)
32. Schiecke K, Schumann A, Benninger F, Feucht M, Baer K-J, Schlattmann P. 2019 Brain–heart interactions considering complex physiological data: processing schemes for time-variant, frequency-dependent, topographical and statistical examination of directed interactions by convergent cross mapping. *Physiol. Meas.* **40**, 114001. (doi:10.1088/1361-6579/ab5050)
33. Catrambone V, Greco A, Vanello N, Scilingo EP, Valenza G. 2019 Time-resolved directional brain–heart interplay measurement through synthetic data generation models. *Ann. Biomed. Eng.* **47**, 1479–1489. (doi:10.1007/s10439-019-02251-y)
34. Ivanov PC, Liu KKL, Bartsch RP. 2016 Focus on the emerging new fields of network physiology and network medicine. *N. J. Phys.* **18**, 100201. (doi:10.1088/1367-2630/18/10/100201)
35. Bashan A, Bartsch RP, Kantelhardt JW, Havlin S, Ivanov PC. 2012 Network physiology reveals relations between network topology and physiological function. *Nat. Commun.* **3**, 702. (doi:10.1038/ncomms1705)
36. Bartsch RP, Liu KKL, Bashan A, Ivanov PC. 2015 Network physiology: how organ systems dynamically interact. *PLoS ONE* **10**, e0142143. (doi:10.1371/journal.pone.0142143)
37. Goldberger AL *et al.* 2000 PhysioBank, PhysioToolkit, and PhysioNet: components of a new research resource for complex physiologic signals. *Circulation* **101**, e215–e220. (doi:10.1161/01.CIR.101.23.e215)
38. Babaeizadeh S, Zhou SH, Pittman SD, White DP. 2011 Electrocardiogram-derived respiration in screening of sleep-disordered breathing. *J. Electrocardiol.* **44**, 700–706. (doi:10.1016/j.jelectrocard.2011.08.004)
39. Pan J, Tompkins WJ. 1985 A real-time QRS detection algorithm. *IEEE Trans. Biomed. Eng.* **BME-32**, 230–236. (doi:10.1109/TBME.1985.325532)
40. Elgendi M, Fletcher R, Liang Y, Howard N, Lovell NH, Abbott D, Lim K, Ward R. 2019 The use of photoplethysmography for assessing hypertension. *npj Digit. Med.* **2**, 60. (doi:10.1038/s41746-019-0136-7)
41. Liang Y, Abbott D, Howard N, Lim K, Ward R, Elgendi M. 2019 How effective is pulse arrival time for evaluating blood pressure? Challenges and recommendations from a study using the MIMIC database. *J. Clin. Med.* **8**, 337. (doi:10.3390/jcm8030337)
42. Liu X, Pamula Y, Kohler M, Baumert M. 2019 A method for estimating pulse wave amplitude variability in children with sleep disordered breathing. In *Proc. 2019 41st Annu. Int. Conf. of the IEEE Engineering in Medicine and Biology Society (EMBC), Berlin, Germany, 23–27 July 2019*, pp. 2289–2292. IEEE.
43. Granger CWJ. 1969 Investigating causal relations by econometric models and cross-spectral methods. *Econometrica* **37**, 424–438. (doi:10.2307/1912791)
44. Porta A, Faes L. 2016 Wiener–Granger causality in network physiology with applications to cardiovascular control and neuroscience. *Proc. IEEE* **104**, 282–309. (doi:10.1109/JPROC.2015.2476824)
45. Bressler SL, Seth AK. 2011 Wiener–Granger causality: a well established methodology. *Neuroimage* **58**, 323–329. (doi:10.1016/j.neuroimage.2010.02.059)
46. Schiatti L, Nollo G, Rossato G, Faes L. 2015 Extended Granger causality: a new tool to identify the structure of physiological networks. *Physiol. Meas.* **36**, 827–843. (doi:10.1088/0967-3334/36/4/827)

47. Porta A, Bassani T, Bari V, Pinna GD, Maestri R, Guzzetti S. 2012 Accounting for respiration is necessary to reliably infer Granger causality from cardiovascular variability series. *IEEE Trans. Biomed. Eng.* **59**, 832–841. (doi:10.1109/tbme.2011.2180379)
48. American Sleep Disorders Association. 1992 ASDA report. EEG arousals: scoring rules and examples. *Sleep* **15**, 173. (doi:10.1093/sleep/15.2.173)
49. Gonzalez-Salazar JS, Alba A, Mendez MO, Luna-Rivera JM, Parrino L, Grassi A, Terzano M, Milioli G. 2014 Characterization of the autonomic system during the cyclic alternating pattern of sleep. In *Proc. 2014 36th Annu. Int. Conf. of the IEEE Engineering in Medicine and Biology Society, Chicago, IL, 26–30 August 2014*, pp. 3805–3808. IEEE.
50. Sforza E, Jouny C, Ibanez V. 2000 Cardiac activation during arousal in humans: further evidence for hierarchy in the arousal response. *Clin. Neurophysiol.* **111**, 1611–1619. (doi:10.1016/S1388-2457(00)00363-1)
51. Trinder J, Waloszek J, Woods MJ, Jordan AS. 2012 Sleep and cardiovascular regulation. *Pflügers Arch. - Eur. J. Physiol.* **463**, 161–168. (doi:10.1007/s00424-011-1041-3)
52. Baumert M, Kohler M, Kabir M, Kennedy D, Pamula Y. 2010 Cardiorespiratory response to spontaneous cortical arousals during stage 2 and rapid eye movement sleep in healthy children. *J. Sleep Res.* **19**, 415–424. (doi:10.1111/j.1365-2869.2009.00798.x)
53. Halász P, Terzano M, Parrino L, Bódizs R. 2004 The nature of arousal in sleep. *J. Sleep Res.* **13**, 1–23. (doi:10.1111/j.1365-2869.2004.00388.x)
54. Terzano MG, Parrino L, Rosa A, Palomba V, Smerieri A. 2002 CAP and arousals in the structural development of sleep: an integrative perspective. *Sleep Med.* **3**, 221–229. (doi:10.1016/S1389-9457(02)00009-6)
55. Bonnet MH, Arand DL. 1997 Heart rate variability: sleep stage, time of night, and arousal influences. *Electroencephalogr. Clin. Neurophysiol.* **102**, 390–396. (doi:10.1016/S0921-884X(96)96070-1)
56. Ferri R, Bruni O, Miano S, Terzano MG. 2005 Topographic mapping of the spectral components of the cyclic alternating pattern (CAP). *Sleep Med.* **6**, 29–36. (doi:10.1016/j.sleep.2004.06.010)
57. Leon-Lomeli R *et al.* 2014 Relation between heart beat fluctuations and cyclic alternating pattern during sleep in insomnia patients. In *Proc. 2014 36th Annu. Int. Conf. of the IEEE Engineering in Medicine and Biology Society, Chicago, IL, 26–30 August 2014*. IEEE.
58. Ding M, Bressler SL, Yang W, Liang H. 2000 Short-window spectral analysis of cortical event-related potentials by adaptive multivariate autoregressive modeling: data preprocessing, model validation, and variability assessment. *Biol. Cybern.* **83**, 35–45. (doi:10.1007/s004229900137)
59. Marinazzo D, Pellicoro M, Stramaglia S. 2008 Kernel method for nonlinear Granger causality. *Phys. Rev. Lett.* **100**, 144103. (doi:10.1103/PhysRevLett.100.144103)
60. McIntosh AR, Gonzalez-Lima F. 1994 Structural equation modeling and its application to network analysis in functional brain imaging. *Hum. Brain Mapp.* **2**, 2–22. (doi:10.1002/hbm.460020104)
61. Winterhalder M, Schelter B, Hesse W, Schwab K, Leistritz L, Klan D, Bauer R, Timmer J, Witte H. 2005 Comparison of linear signal processing techniques to infer directed interactions in multivariate neural systems. *Signal Processing* **85**, 2137–2160. (doi:10.1016/j.sigpro.2005.07.011)
62. Barrett A, Barnett L. 2013 Granger causality is designed to measure effect, not mechanism. *Front. Neuroinform.* **7**, 6. (doi:10.3389/fninf.2013.00006)
63. Greco A, Faes L, Catrambone V, Barbieri R, Scilingo EP, Valenza G. 2019 Lateralization of directional brain-heart information transfer during visual emotional elicitation. *Am. J. Physiol. Integr. Comp. Physiol.* **317**, R25–R38. (doi:10.1152/ajpregu.00151.2018)
64. Faes L, Marinazzo D, Stramaglia S, Jurysta F, Porta A, Giandomenico N. 2016 Predictability decomposition detects the impairment of brain–heart dynamical networks during sleep disorders and their recovery with treatment. *Phil. Trans. R. Soc. A* **374**, 20150177. (doi:10.1098/rsta.2015.0177)
65. Hartmann S, Baumert M. 2019 Automatic A-phase detection of cyclic alternating patterns in sleep using dynamic temporal information. *IEEE Trans. Neural Syst. Rehabil. Eng.* **27**, 1695–1703. (doi:10.1109/TNSRE.2019.2934828)

66. Hartmann S, Bruni O, Ferri R, Redline S, Baumert M. 2020 Characterization of cyclic alternating pattern during sleep in older men and women using large population studies. *Sleep* **43**, zsaa016. (doi:10.1093/sleep/zsaa016)
67. Hartmann S, Bruni O, Ferri R, Redline S, Baumert M. 2020 Cyclic alternating pattern (CAP) in children with obstructive sleep apnea and its relationship with adenotonsillectomy, behavior, cognition, and quality-of-life. *Sleep* **44**, zsaa145. (doi:10.1093/sleep/zsaa145)
68. Parrino L, Boselli M, Spaggiari MC, Smerieri A, Terzano MG. 1998 Cyclic alternating pattern (CAP) in normal sleep: polysomnographic parameters in different age groups. *Electroencephalogr. Clin. Neurophysiol.* **107**, 439–450. (doi:10.1016/S0013-4694(98)00108-4)
69. Hirshkowitz M. 2002 Arousals and anti-arousals. *Sleep Med.* **3**, 203–204. (doi:10.1016/S1389-9457(02)00018-7)
70. Bruni O, Novelli L, Miano S, Parrino L, Terzano MG, Ferri R. 2010 Cyclic alternating pattern: a window into pediatric sleep. *Sleep Med.* **11**, 628–636. (doi:10.1016/j.sleep.2009.10.003)